The C-terminal Ca2+-binding domain of SPARC confers anti-spreading activity to human urothelial cells

ARTICLE *in* JOURNAL OF CELLULAR PHYSIOLOGY · JANUARY 2006

Impact Factor: 3.84 · DOI: 10.1002/jcp.20462 · Source: PubMed

5 AUTHORS, INCLUDING:

James Bassuk
Seattle Children's Research Institute
53 PUBLICATIONS **1,616** CITATIONS

JOURNAL OF CELLULAR PHYSIOLOGY 206:211–220 (2006)

The C-Terminal Ca^{2+}-Binding Domain of SPARC Confers Anti-Spreading Activity to Human Urothelial Cells

CATHERINE F. DELOSTRINOS,[1,2] AMBER E. HUDSON,[1] WALDO C. FENG,[1] JEFFREY KOSMAN,[1,2] AND JAMES A. BASSUK[1,2]*

[1]*Program in Human Urothelial Biology, Children's Hospital and Regional Medical Center, Seattle, Washington*
[2]*Department of Urology, University of Washington School of Medicine, Seattle, Washington*

The anti-spreading activity of secreted protein acidic and rich in cysteine (SPARC) has been assigned to the C-terminal third domain, a region rich in α-helices. This ''extracellular calcium-binding'' (EC) domain contains two EF-hands that each coordinates one Ca^{2+} ion, forming a helix-loop-helix structure that not only drives the conformation of the protein but is also necessary for biological activity. Recombinant (r) EC, expressed in *E. coli*, was fused at the C-terminus to a His hexamer and isolated under denaturing conditions by nickel-chelate affinity chromatography. rEC-His was renatured by procedures that simultaneously (i) removed denaturing conditions, (ii) catalyzed disulfide bond isomerization, and (iii) initiated Ca^{2+}-dependent refolding. Intrinsic tryptophan fluorescence and circular dichroism spectroscopies demonstrated that rEC-His exhibited a Ca^{2+}-dependent conformation that was consistent with the known crystal structure. Spreading assays confirmed that rEC-His was biologically active through its ability to inhibit the spreading of freshly plated human urothelial cells propagated from transitional epithelium. rEC-His and rSPARC-His exhibited highly similar anti-spreading activities when measured as a function of concentration or time. In contrast to the wild-type and EC recombinant proteins, rSPARC(E268F)-His, a point substitution mutant at the Z position of EF-hand 2, failed to exhibit both Ca^{2+}-dependent changes in α-helical secondary structure and anti-spreading activity. The collective data provide evidence that the motif of SPARC responsible for anti-spreading activity was dependent on the coordination of Ca^{2+} by a Glu residue at the Z position of EF-hand 2 and provide insights into how adhesive forces are balanced within the extracellular matrix of urothelial cells. J. Cell. Physiol. 206: 211–220, 2006. © 2005 Wiley-Liss, Inc.

The inner surface of the lower urinary tract is lined with transitional epithelial tissue, or urothelium, that functions as a barrier to microorganisms, toxins, and the highly variable waste products in urine. All major diseases of the bladder involve the urothelium. Such diseases include urothelial cancer, urinary tract infection, interstitial cystitis, and developmental abnormalities such as vesicoureteral reflux and exstrophy. Knowledge of the mechanism by which the urothelium repairs itself is, therefore, necessary in determining the factors that cause various afflictions of the lower urinary tract.

Interactions between urothelial cells and their underlying extracellular matrix are major determinants of cell shape, progression through the cell cycle, migration, and differentiation (Hay, 1981; Adams and Watt, 1993; Ingber, 1993; Juliano and Haskill, 1993). The urothelial basement membrane and extracellular matrix together form an adhesive substratum that facilitates attachment, spreading, and the formation of focal adhesions (Gumbiner, 1996). How urothelial cells spread is central to understanding a number of bladder diseases. The extracellular matrix-associated secreted protein acidic and rich in cysteine (SPARC), also known as BM-40 and osteonectin (Termine et al., 1981; Romberg et al., 1985), has been shown to inhibit the spreading of human urothelial cells derived from embryologically distinct origins in concentration- and time-dependent processes (Hudson et al., 2005). Such inhibitory activity provides a mechanism in which SPARC can modulate the interactions between basal urothelial cells and the urothelial basement membrane.

Human SPARC is a multi-functional protein that is comprised of three major domains. A 53-residue domain I follows a 17-residue N-terminal secretory signal sequence and contains two clusters of Glu residues that bind Ca^{2+} ions with high-capacity and low affinity (Engel et al., 1987; Maurer et al., 1992). Domain II is comprised of two sub-domains: a 24-residue follistatin-like

Abbreviations: SPARC, secreted protein acidic and rich in cysteine; EC, extracellular calcium binding; TGF, transforming growth factor; PCR, polymerase chain reaction; IPTG, isopropylthiogalactopyranoside; SDS–PAGE, polyacrylamide gel electrophoresis that contains 0.1% sodium dodecyl sulfate; Ni-NTA, nickel-chelate nitrilotriacetic acid; DTT, dithiothreitol; PVDF, polyvinylidene difluoride; CAPS, 3-[cyclohexylamino]-1-propanesulfonic acid; GSH, reduced glutathione; GSSG, oxidized glutathione; rSPARC-His, recombinant SPARC that contains a C-terminal hexamer of histidine residues; rEC-His, the recombinant EC-domain of SPARC that contains a C-terminal hexamer of histidine residues; rSPARC(E268F)-His, recombinant SPARC with a substitution of a F residue for E at position 268.

Contract grant sponsor: Howard Hughes Undergraduate Research Program; Contract grant sponsor: Mary Gates Endowment for Students Research Training Grant; Contract grant sponsor: NIDDK; Contract grant numbers: T32 DK07779, R01DK58881; Contract grant sponsor: Residency Review Committee for Urology.

Waldo C. Feng's present address is Children's Urology Associates, Las Vegas, Nevada, 89109.

*Correspondence to: James A. Bassuk, Division of Pediatric Urology, Children's Hospital and Regional Medical Center, 4800 Sand Point Way NE, P.O. Box 5371/Mail Stop A-8938, Seattle, WA, 98105-0371. E-mail: james.bassuk@seattlechildrens.org

Received 27 December 2004; Accepted 22 April 2005

DOI: 10.1002/jcp.20462

region (Shibanuma et al., 1993) and a 55-residue serine protease-like inhibitor region (Bolander et al., 1988). The third domain is an extracellular Ca^{2+}-binding region termed the "EC" domain (Maurer et al., 1995; Hohenester et al., 1996) and is comprised of the C-terminal 151 residues. The structure of the EC domain has been solved and shown to be an autonomously folding domain that binds Ca^{2+} and collagen (Maurer et al., 1995; Hohenester et al., 1996). The prediction of two Ca^{2+}-binding EF hands in the EC domain (Bassuk et al., 1993) was confirmed by the crystal structure of SPARC (Hohenester et al., 1996). These two Ca^{2+}-binding motifs are distinguished from cytosolic EF-hands because (i) insertion of one amino acid residue into the loop of the first EF-hand induces a Ca^{2+} coordination variant and (ii) a disulfide bond connects the helices of the second EF-hand (Hohenester et al., 1996). These two EF-hands bind Ca^{2+} cooperatively and with high affinity (Busch et al., 2000), suggesting that the EF-hands of SPARC function in a structural rather than a regulatory role. The collagen-binding site of SPARC has been mapped to the EC domain, in agreement with the structural requirement for Ca^{2+} for this interaction (Maurer et al., 1995; Sasaki et al., 1998). SPARC was recently reported to inhibit epithelial cell proliferation by selectively commandeering the TGF-β signaling system, doing so through coupling of the EC-domain of SPARC to a TGF-β receptor- and Smad2/3-dependent pathway (Schiemann et al., 2003).

To better understand the mechanisms and structural/functional relationships of how SPARC inhibits the spreading of human urothelial cells, we have engineered, expressed, and isolated recombinant preparations of human wild-type SPARC and its EC domain from *Escherchia coli*. Preparations of recombinant EC were found to exhibit secondary structures and biological activities consistent with the properties of native and recombinant SPARC from both bacterial and mammalian cells (Sage et al., 1989; Lane and Sage, 1994; Yost et al., 1994; Motamed et al., 1995; Bassuk et al., 1996a,b) as well as recombinant EC from mammalian cells (Schiemann et al., 2003). Through a quantitative spreading assay, the anti-spreading activity of SPARC was assigned to the EC domain. This activity was lost with the disruption of the second Ca^{2+}-binding EF hand by site-directed mutagenesis. The elucidation of the structural domains of SPARC and of the requirement for occupation of high-affinity Ca^{2+} sites, for anti-spreading activity, advances the field of urothelial cell biology and provides realistic targets for therapeutic intervention in the management of a variety of urinary tract conditions.

MATERIALS AND METHODS

Materials

Oligonucleotide primers were generated at Biosource International (Camarillo, CA). Plasmid pET22b, *E. coli* strains NovaBlue and BL21(DE3) competent cells, T7 promoter and terminator primers, BugBuster Protein Extraction Reagent, and carbenicillin were all purchased from Novagen (Madison, WI). GeneAmp PCR Reagent Kit, isopropylthiogalactopyranoside (IPTG), and Complete Protease Inhibitor Cocktail Tablets were purchased from Roche Diagnostic Corp (Indianapolis, IN). Restriction enzymes *Sma*I, *Nde*I, and *Xho*I as well as T4 DNA ligase were purchased from MBI Fermentas (Hanover, MD). SYBR Green was obtained from Molecular Probes (Eugene, OR). QIAquick Gel Extraction Kit, Plasmid Mini Kit, and Ni-NTA metal chelate affinity resin were purchased from QIAGEN, Inc. (Chatsworth, CA). Chelex 100 Resin was purchased from Bio-Rad Laboratories, Inc. (Hercules, CA). Microcon-10 centrifugal microconcentrators were purchased from Amicon (Bedford, MA). Anti-His C-term mouse immunoglobulin conjugated to horseradish peroxidase (R930-25), HEPES buffer, Hank's Balanced Salt Solution, and Defined Keratinocyte Serum-Free Medium (DK-SFM) were obtained from Invitrogen (Carlsbad, CA). QuikChange site-directed mutagenesis kit was purchased from Stratagene (La Jolla, CA). Image Pro Plus 5.0 software was purchased from Media Cybernetics (Silver Springs, MD).

Construction of recombinant plasmid encoding EC domain

Plasmid pSPARCwt, a pET22b plasmid harboring the cDNA sequence encoding the mature, secreted form of human SPARC (Bassuk et al., 1996a), was used as a template for the *Taq* polymerization of the EC domain. One pair of oligonucleotide primers was synthesized: ECNde1, 5′-CATCCGGATCATATGGCCCCCCCTTGCCTGGAC-3′, and 3202, 5′-ACTCTCCGGCTACTCGAGGATCACAAGATCCTTG-3′. These oligonucleotide primers were 33 and 34 bases in length, respectively, and were designed to partially anneal to the region flanking the EC domain of SPARC. The oligonucleotide primer ECNde1 conferred the recognition site for the restriction endonuclease *Nde*I 5′ to the first translation codon (Ala) of the EC domain PCR-DNA product. Oligonucleotide primer 3202 conferred the site for *Xho*I at the 3′ end of the EC domain PCR-DNA product. PCR was performed using one unit of *Taq* polymerase for one cycle (95°C, 12 min), 40 cycles (95°C, 1 min; 50°C, 1 min; and 72°C, 1 min), and one cycle (72°C, 12 min). Ten microliters of the 50 μl resultant PCR product was resolved by electrophoresis through a 2% agarose gel in 40 mM Tris-acetate (pH 8.0) and 1 mM ethylenediaminetetraacetic acid (EDTA) and stained in 0.2 μl/ml of SYBR Green for 1 h, yielding a 500 bp band. Six microliters of the remaining PCR product was re-amplified. Subsequent agarose gel electrophoresis yielded the 500 bp band, which was cut out and extracted using Qiagen's QIAquick Gel Extraction Kit. A fraction of the extracted band was digested with *Sma*I, and upon gel electrophoresis a doublet of approximately 250 bp was obtained, indicating that the middle of the EC domain DNA was intact. The PCR-DNA product and the bacterial expression plasmid pET-22b were each digested with *Nde*I and *Xho*I and joined with T4 ligase to form the recombinant plasmid pET22b-EC. This recombinant plasmid was transformed into NovaBlue Competent Cells, which were plated onto Luria-Bertani (LB) broth agar plates containing 50 μg/ml carbenicillin, 12.5 μg/ml tetracycline, and 0.2% glucose and incubated at 37°C overnight. Growth of wild-type cells was selected against by the inclusion of carbenicillin (50 μg/ml) and tetracycline (12.5 μg/ml) in all plates and media by the resistance conferred by the recombinant plasmid and NovaBlue strain, respectively. Isolated recombinant colonies were used to culture 25 and 15 ml of LB broth for glycerol stocks and plasmid DNA extraction. Qiagen's MiniPrep Kit was used to isolate the pET22b-EC plasmid DNA. Dideoxy sequencing of the supercoiled plasmid DNA was determined with an Applied Biosystem's ABI3730XL DNA sequencer using T7 promoter primers.

Growth and expression of recombinant EC domain in *E. coli*

Competent BL21(DE3) *E. coli* cells were transformed with the isolated pET22b-EC domain plasmid. The cells were plated and growth of wild-type cells was selected against by inclusion of carbenicillin (50 μg/ml) in all plates and media by the resistance conferred by the recombinant plasmid. Isolated colonies were restreaked and incubated at 37°C overnight. From this plate, an isolated colony was used to grow a 25-ml culture in LB broth containing the appropriate selective antibiotics for glycerol stocks. Stable cultures in the following procedures were propagated from frozen glycerol stocks.

Cells were grown on LB agar plates with carbenicillin (50 μg/ml) and 0.2% glucose at 37°C overnight. An isolated colony was used to inoculate a 25 ml LB culture containing carbenicillin (50 μg/ml) and 0.2% glucose, which was grown at 37°C in a shaking incubator at 105 rpm until the optical density at 600 nm reached approximately 0.8. EC domain RNA synthesis

was induced by the addition of IPTG to a final concentration of 1 mM. The culture grew for an additional 3 h, during which 1 ml samples were retrieved for total cell lysate analysis. SDS–PAGE analysis on a 15% polyacrylamide gel revealed an induced band occurring at 18 kDa, the molecular weight of the EC domain protein.

Large-scale inductions were performed to increase the recombinant EC domain protein yield. Isolated colonies obtained from LB broth agar streak plates of glycerol stocks were used to inoculate a 100-ml starter culture of LB broth, carbenicillin (50 μg/ml), and 0.2% glucose. The starter culture was grown at 37°C at 100 rpm to mid-log exponential phase ($OD_{600} = 0.8$) and stored overnight at 4°C. The following day, cells were collected via centrifugation at 5,000*g*, resuspended in identical culture medium, and used to inoculate four 500 ml cultures. Once grown at 37°C at 90 rpm to mid-log exponential phase, the cultures were induced with IPTG. After 3 h, the cells were collected via centrifugation at 5,000*g*, resuspended in 50 ml of 100 mM NaCl, 10 mM Tris-HCl (pH 8.0), and 1 mM EDTA and centrifuged again at 5,000*g*. The resulting pellet was frozen and stored at −20°C.

Solubility and purification of recombinant EC domain

Cells obtained from induction were used to determine the solubility of the recombinant EC domain. The cells were lysed using Bug Buster protein extraction reagent with the addition of Complete Protease Inhibitor Cocktail Tablets. Cellular lysates were separated into 4 equal parts, centrifuged at 16,000*g*, and the soluble fraction was removed. To each of the insoluble pellets, a solution of 0.1 M NaH_2PO_4, 0.5 M NaCl, and 0.05 M Tris-HCl (pH 8.0) that contained 1, 2, 4, or 8 M urea was added. After incubation at ambient temperature for 2 h with frequent vortexing, insoluble material was removed by sedimentation at 16,000*g*, supernatants were recovered, and solubilized proteins were fractionated by 15% polyacrylamide gels that contained 0.1% SDS (SDS–PAGE). Quantification of individual bands was accomplished using the line profile function of Image Pro Plus 5.0 software on a scanned image of the gel. The relative intensity of the 18 kDa rEC-His band was plotted as a function of the urea concentration.

The recombinant EC domain was isolated by nickel-chelate nitrilotriacetic acid (Ni-NTA) affinity chromatography. The column was allowed to settle at 1*g* for 1 h, and then packed at 2.66 ml/min. Bacterial paste obtained from a 2 L induction was denatured in 6 M guanidine hydrochloric acid, 0.1 M NaH_2PO_4, 0.05 M Tris-HCl (pH 8.0), and 0.5 M NaCl and centrifuged at 14,000*g* to obtain a supernate free of insoluble debris. Imidazole was added to the supernate to a final concentration of 0.025 M to prevent non-specific binding of bacterial proteins to the nickel resin. The column was washed at 2 ml/min with buffer A (8 M urea, 0.1 M NaH_2PO_4, 0.5 M NaCl, 0.05 M Tris-HCl) at pH 8.0 for 1 h. Proteins that remained non-specifically bound to the resin were removed with buffer A at pH 6.0 until the absorbance at 280 nm is <0.01 OD. rEC-His was then eluted with buffer A at pH 4.5, with collections taken at 10 ml per fraction at a rate of 2 ml/min. The fraction collector, rate of elution, optical density and pH of the elutant, and administration of buffers were controlled by an Amersham AKTA Purifier High Performance Liquid Chromatography Unit. A sample of the proteins eluted at pH 4.5 was diluted with an equal volume of water and precipitated with 10% (w/v) trichloroacetic acid. Samples were dissolved in sample buffer that contained or lacked 0.1 M dithiothreitol (DTT) and analyzed by SDS–PAGE. The isolated protein was transferred to a polyvinylidene difluoride (PVDF) membrane in 0.01 M CAPS (pH 11.0) and 20% methanol for 1 h at 0.43 A. The transferred protein was stained in Coomassie Blue R-250 for visualization, and subjected to N-terminal amino acid sequencing by Edman degradation.

Renaturation of rEC-His

The proteins eluted at pH 4.5 of buffer A were refolded with a sequence of buffers that removed denaturing conditions and introduced conditions known to aid in correct refolding. The proteins were first dialyzed at ambient temperature in buffer 1 (8 M urea, 0.1 M NaH_2PO_4, 0.5 M NaCl, and 0.05 M Tris-HCl) at pH 8.0 to increase the pH of the sample. The sample was then dialyzed at 4°C in buffer 2 (0.1 M NaH_2PO_4, 0.5 M NaCl, and 0.05 M Tris-HCl, pH 8.5) and subsequently at 4 °C in buffer 3 (0.5 M NaCl, 0.05 M Tris-HCl, pH 8.5) to remove urea and phosphate, respectively. After dialysis, reduced (GSH) and oxidized (GSSG) glutathione were added to final concentration of 1×10^{-3} and 2×10^{-5} M, respectively, to facilitate isomerization of disulfide bonds. $CaCl_2$ was added to a final concentration of 0.01 M to induce folding and generation of α-helices. Assessment of isomerization and refolding was achieved by SDS–PAGE after samples were centrifugally concentrated and treated with and without DTT.

Construction of recombinant plasmid encoding the rSPARC(E268F)-His mutant

The codon for E268 was replaced with a codon for F through use of a QuikChange site-directed mutagenesis kit. The following oligonucleotide primer pair, 5′-CATCGCCCTG-GATTTCTGGGCCGGCTGC-3′ and 5′-GCAGCCGGCCCA-GAAATCCAGGGCGATG-3′, was annealed to a pSPARCwt template. Extension was achieved with *Pfu* DNA polymerase. Residual template DNA was preferentially digested away with *Dpn*I restriction endonuclease, thereby allowing mutation-containing DNA to survive transformation and growth in *E. coli*. Dideoxy-sequencing of both strands across the coding region verified the mutation.

Expression, isolation, and renaturation of rSPARC(E268F)-His

The mutant protein was expressed in an analogous manner as wild-type rSPARC-His (Bassuk et al., 1996a,b). In some preparations, recombinant protein was produced by fermentation (Schneider et al., 1997). Renaturation was accomplished by the column-refolding method (Bassuk et al., 1996b) or by the dialysis-refolding method described above for rEC-His.

Fluorescence emission spectroscopy

Fluorescence measurements were performed in a Perkin-Elmer LS-50B luminescence spectrometer. Renatured rEC-His and rSPARC(E268F)-His were dialyzed into buffer that contained 50 mM Tris-HCl (pH 8.0) and 150 mM NaCl. The samples were diluted into a final protein concentration of 37.5 μg/ml (rEC-His) or 40 μg/ml (rSPARC(E268F)-His), placed in a cuvette (pathlength = 1 cm), and excited at 280 nm. Emission intensities were monitored from 300 to 500 nm at a scan speed of 200 nm/min. Resolution slit widths were 6 nm for excitation and 7 nm for emission. Spectra were obtained of samples with increasing concentrations of EDTA (0.0–2.5 mM) or $CaCl_2$ (0.0–5.0 mM). All measurements were performed at ambient temperature, and the spectra of solutions containing no protein were subtracted from those containing protein.

Circular dichroism spectroscopy

Proteins were dialyzed overnight in Chelex-treated buffer that contained 150 mM NaCl and 50 mM Tris-HCl (pH 8.5) to remove glutathione and unbound Ca^{2+} ions. After dilution to a final concentration of 250 (rSPARC-His), 170 (rEC-His), or 300 μg/ml (rSPARC(E268F)-His), the sample was placed in a quartz cell (pathlength = 0.1 cm) and scanned from 260 to 190 nm at ambient temperature in an Aviv 62DS or a Jasco J-715 circular dichroism spectropolarimeter. Spectra were obtained from samples with increasing concentrations of EDTA (0.0–2.5 mM) or $CaCl_2$ (0.0–5.0 mM). Spectra of Chelex-treated buffer were subtracted from the spectra of the protein. Six scanning spectra were averaged and the data were smoothed ±2 points with the moving average algorithm. The mean residue molar ellipticity was calculated by using the mean residue molecular mass as 110 Da.

Western immunoblotting

Proteins were fractionated by 15% SDS–PAGE and transferred to nitrocellulose membranes of 0.2 μm porosity at 130 V for 1 h in 25 mM Tris-HCl (pH 8.3), 192 mM glycine, and 20% methanol. The membranes were treated with mouse monoclonal antibodies specific for C-terminal His_{6x} conjugated to

horseradish peroxidase. Visualization was achieved by enhanced chemical luminescence.

Urothelial cells

Bladder and ureteric tissue was obtained, with informed consent, as surgical explants under a human subjects protocol approved by the Institutional Review Board of Children's Hospital and Regional Medical Center. Urothelial cells were derived from the following tissue: normal bladder transitional epithelia of a 13-year female that presented with vesicoureteral reflux; normal ureteric transitional epithelia from a 2-month female that presented with a dilated ureter due to an obstruction at the junction of the ureter and renal pelvis.

Spreading assays

Refolded proteins were dialyzed overnight against 1× Hank's Balanced Salt Solution (HBBS) that contained 10 mM HEPES (pH 7.4). A primary culture of human urothelial cells was grown in Defined Keratinocyte Serum-Free Medium at 37°C in a humidified incubator that contained 5% CO_2. Just prior to confluency, the cells were trypsinized, counted, and replated at a density of $1-2 \times 10^3$ cells/well of a 24-well plate. Contained within the plate were varying concentrations of rSPARC-His, rEC-His, or rSPARC(E268F)-His. Photographs were taken at 0, 2, 4, 6, and 24 h post plating with a Leica DC200 digital camera. A spreading assay (Bassuk et al., 1996b) was used to quantify the shape of individual cells by calculation of a Rounding Index (RI) according to the following formula: $RI = [(3 \times a) + (2 \times b) + (1 \times c)]/(a + b + c)$. Highly refractile round cells were assigned to the "a" group; fully spread cells were assigned to the "c" group; and cells between round and spread were assigned to the "b" group. A score of 3 represented a culture with only round cells, whereas a score of 1 represented a fully spread culture.

Statistical analyses

P-values were calculated from two-sided, independent-sample Student's *t*-tests that compared the change in rounding indices between groups over the specified time interval (Miller, 1986).

RESULTS

Construction of recombinant plasmid encoding the EC domain of SPARC

The pSPARCwt plasmid has been previously sequenced and shown to encode and express the mature, secreted form of human SPARC (Bassuk et al., 1996a,b). Oligonucleotide primers were designed that integrated *Nde*I and *Xho*I restriction endonuclease sites into 5′ ends of the primers. Using pSPARCwt plasmid as a template, the annealing of these primers and subsequent *Taq* polymerization resulted in PCR-DNA products in which a 500 bp band was the principal component (data not shown). This 500 bp PCR-DNA product was digested with *Nde*I and *Xho*I restriction endonucleases and ligated into pET22b to form the recombinant plasmid vector named pET22b-EC. Dideoxy sequencing of both strands of the insert region of pET22b-EC showed it to be 100% identical to the C-terminal extracellular calcium-binding domain of SPARC (Maurer et al., 1995; Hohenester et al., 1996) and in the proper reading frame for expression. The N-terminus of the recombinant EC domain was predicted to contain an extra Met amino acid, which creates a necessary initiation codon for the bacterial translational machinery. The C-terminus of the recombinant EC domain was predicted to contain eight additional amino acids: Leu, Glu, and $(His)_6$. The Leu and Glu residues are a result of ligation of the EC domain into the *Xho*I restriction site of pET22b. The six His residues were engineered to provide a high-affinity metal-chelation site for purification and antibody detection. The recombinant EC protein fused to His_{6x} was designated as rEC-His.

Growth, expression, and solubility of rEC-His in *E. coli*

Induction of rEC-His was dependent on the addition of IPTG (Fig. 1), a characteristic of the expression system that requires inactivation of the *lac* repressor, induction of the synthesis of chromosomally encoded T7 RNA polymerase under *lac*UV5 control, and subsequent transcription of rEC-His mRNA from its T7 promoter. Figure 1 shows a pattern of protein expression in which the expression of the 18 kDa rEC-His was dependent on IPTG and was a major protein in the total cell lysate.

The total cell lysate of IPTG-induced recombinant *E. coli* culture was separated into soluble and insoluble components. The presence of the large 18 kDa band in the insoluble component (Fig. 2, lane 4) and the absence of the 18 kDa band in the soluble component (Fig. 2, lane 5) indicated that the protein is not soluble under normal expression conditions.

Parallel aliquots of the insoluble fraction were denatured with increasing concentrations of urea and fractionated by SDS–PAGE. The relative extent of solubilized rEC-His at different concentrations of urea was quantified from the intensity values of the 18 kDa band in each lane of the gel (Fig. 3). A 4.3- and 7.9-fold increase of solubilized rEC-His was realized from the dissolution of the sample with 4 and 8 M urea, respectively.

Isolation of denatured rEC-His

The rEC-His polypeptide was isolated from denatured bacterial cell lysates by chromatography on a nickel-chelate resin utilizing the high affinity for nickel of the His hexamer (Hochuli et al., 1987; Hochuli, 1990; Crowe et al., 1994; Bassuk et al., 1996a,b) engineered onto the C-terminus of the recombinant polypeptide. Contaminating bacterial proteins that failed to interact with the resin due to their lower affinity (Hochuli et al., 1987)

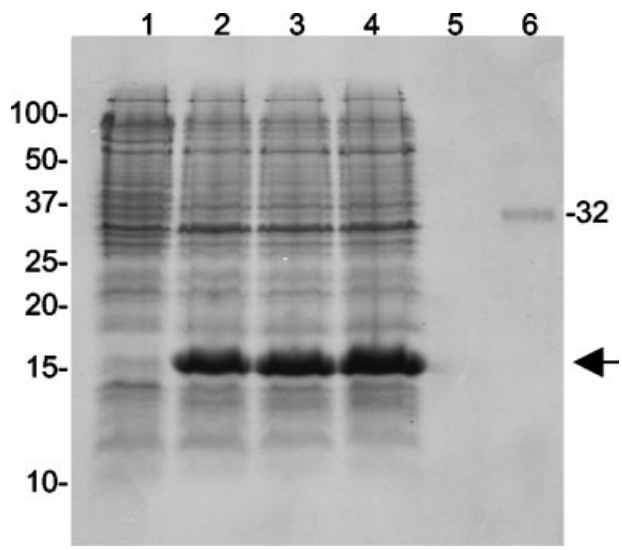

Fig. 1. Expression of recombinant EC domain in *E. coli*. Shown is a Coomassie Blue R-250 stained polyacrylamide SDS gel of 1 ml samples taken at hourly intervals during growth of a 2 L culture. Molecular weight markers with M_r to the left of the figure. Lane 1, 0 h sample prior to induction. Lane 2, 1 h post induction. Lane 3, 2 h post induction. Lane 4, 3 h post induction. Lane 5, blank. *Arrow*, putative rEC-His. Lane 6, 32 kDa rSPARC-His standard.

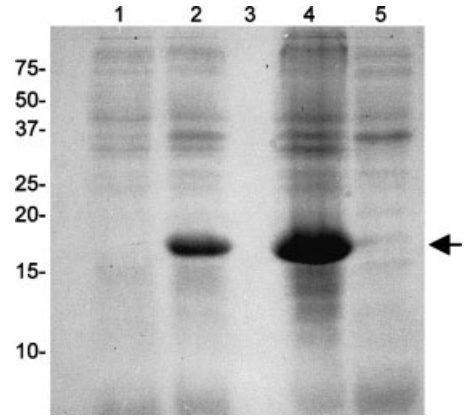

Fig. 2. Partitioning of rEC-His into the insoluble fraction of *E. coli* extracts. Shown is a Coomassie Blue R-250 stained 15% polyacrylamide gel that contained 0.1% SDS. Sizes in kDa are shown to the left of the figure. Lane 1, total protein sample from a culture not induced with IPTG. Lane 2, total protein sample from a culture 3 h after induction with IPTG. Lane 3, blank. Lane 4, insoluble fraction from a culture 3 h after induction with IPTG. Lane 5, soluble fraction from a culture 3 h after induction with IPTG. Arrow, electrophoretic mobility of the 18 kDa rEC-His.

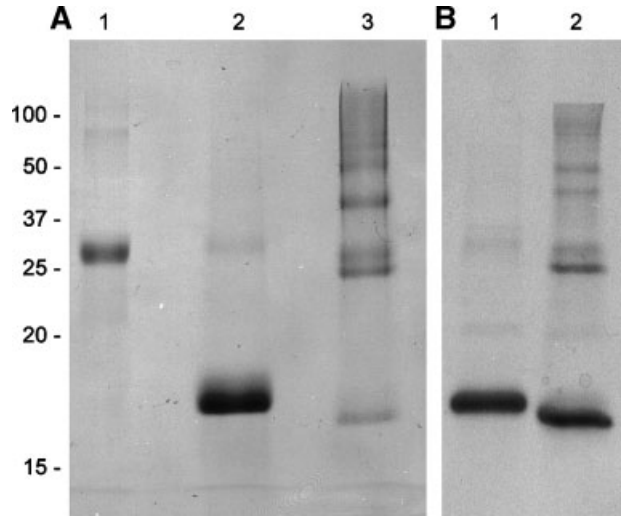

Fig. 4. Isolation and renaturation of rEC-His. Shown are Coomassie Blue R250-stained polyacrylamide SDS gels. Sizes in kDa are shown to the left of the figure. **A**: Isolation by Ni-NTA chromatography. Lane 1, 32 kDa rSPARC-His standard. Lane 2, fraction from pH 4.5 elution and reduced with DTT prior to electrophoresis. Lane 3, fraction from pH 4.5 elution, not reduced. The major component of pH 4.5 elution fraction is the 18 kDa rEC-His. **B**: Shift in electrophoretic mobility distinguishes the oxidized and reduced forms of renatured rEC-His. Lane 1, reduction of renatured rEC-His by DTT. Lane 2, renatured rEC-His under non-reducing conditions.

were removed by washing the column at pH 6.0. Proteins that were bound specifically were eluted at pH 4.5—fractions from this elution were analyzed by SDS–PAGE. Figure 4A shows the properties of rEC-His under reduced (lane 2) and unreduced conditions (lane 3). The 18 kDa monomeric form of rEC-His was the major protein in the pH 4.5 eluate.

Renaturation of rEC-His

Our strategy to facilitate the renaturation of rEC-His involved the removal of denaturing reagents by dialysis and isomerization of disulfide bonds. This strategy was derived, in part, from prior work in our laboratory (Bassuk et al., 1996a) in which we demonstrated that refolding of denatured rSPARC-His into a biologically active form required Ca^{2+} and a glutathione-dependent redox cycle. Since sodium phosphate was a component of chromatography buffers used during the isolation of rEC-His, it was necessary to remove phosphate from the system before the calcium was added to prevent the formation of a calcium phosphate precipitate. SDS–PAGE fractionation was used to evaluate to what extent the renaturation strategy was successful. Figure 4B (lanes 1 and 2) displays the relative electrophoretic mobilities of reduced and unreduced rEC-His, respectively. The observation that the unreduced form of rEC-His (Fig. 4B, lane 2) exhibited a greater relative electrophoretic mobility than the reduced form (Fig. 4B, lane 1) demonstrates that rEC-His was refolded correctly. This observed shift in relative electrophoretic mobility is consistent with prior observations for wild-type and recombinant SPARC proteins (Bassuk et al., 1996a,b; Schneider et al., 1997).

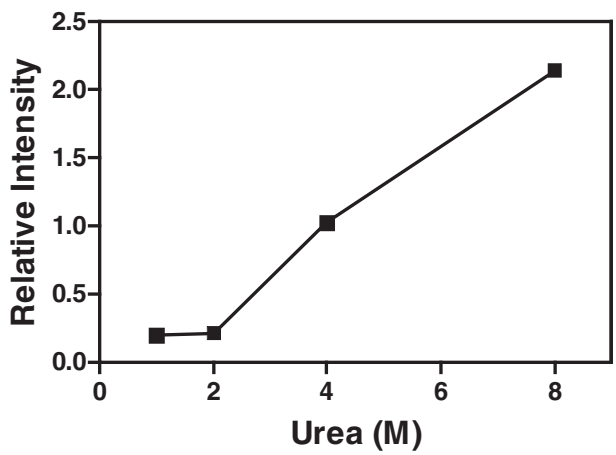

Fig. 3. Solubilization of rEC-His with varying concentrations of urea. The relative intensities were determined from a line profile graph of the Coomassie Blue R250-stained 18 kDa band from a 15% polyacrylamide gel that contained 0.1% SDS.

Amino acid sequence analysis of rEC-His

A preparation of rEC-His was subjected to N-terminal amino acid sequencing by Edman degradation (Edman and Begg, 1967). A mixture of three sequences was obtained: M-A-P-P-L-(C)-D-S-E, A-P-P-L-(C)-D-S-E, and P-P-L-(C)-D-S-E, all of which are consistent with bacterial translational processes (Schmitt et al., 1996). The first step in the isolation of rEC-His was the dissolution of total bacterial protein with 6 M guanidine HCl. This step effectively captured proteins at all stages of nascent translation and post-translational processing, including forms of rEC-His with the N-formyl-Met and N-formyl-Met-Ala sequence still yet to be cleaved from bacterial mono- and di-peptidases (Schmitt et al., 1996). The sequences obtained from Edman degradation are in agreement with the N-terminal sequence that we predicted from the cDNA sequence (Bassuk et al., 1996a) and with a prior report on the crystal structure of the EC domain (Hohenester et al., 1996). We conclude that our preparations of rEC-His are intact because (i) the N-terminal sequence is correct and (ii) the C-terminal His hexamer is functional due to the ability of rEC-His to interact with nickel-chelate affinity resins (Fig. 4A) and with anti-His(C-term) antibodies (data not shown).

Fluorescence emission spectroscopy of renatured rEC-His

To determine if the interaction of Ca^{2+} with rEC-His would influence its conformation, the renatured polypeptide was subjected to intrinsic fluorescence emission spectroscopy. Preparations of rEC-His for this assay involved saturation of rEC-His with Ca^{2+} followed by extensive dialysis to remove unbound Ca^{2+}. Under these conditions, rEC-His exhibited an emission maximum of 335 nm (Fig. 5A, solid line), indicating a relatively sheltered environment for the three Trp residues residing in this domain of SPARC (Bassuk et al., 1996b; Hohenester et al., 1996; Davidson et al., 1999). Bound Ca^{2+} was removed with addition of increasing concentrations of EDTA (0.0–2.5 mM). Spectra of rEC-His at 0 and 0.0025 mM EDTA were indistinguishable (data not shown). The emission maxima and relative fluorescence intensity increased with EDTA, indicating that rEC-His had become denatured (Fig. 5A, dotted line).

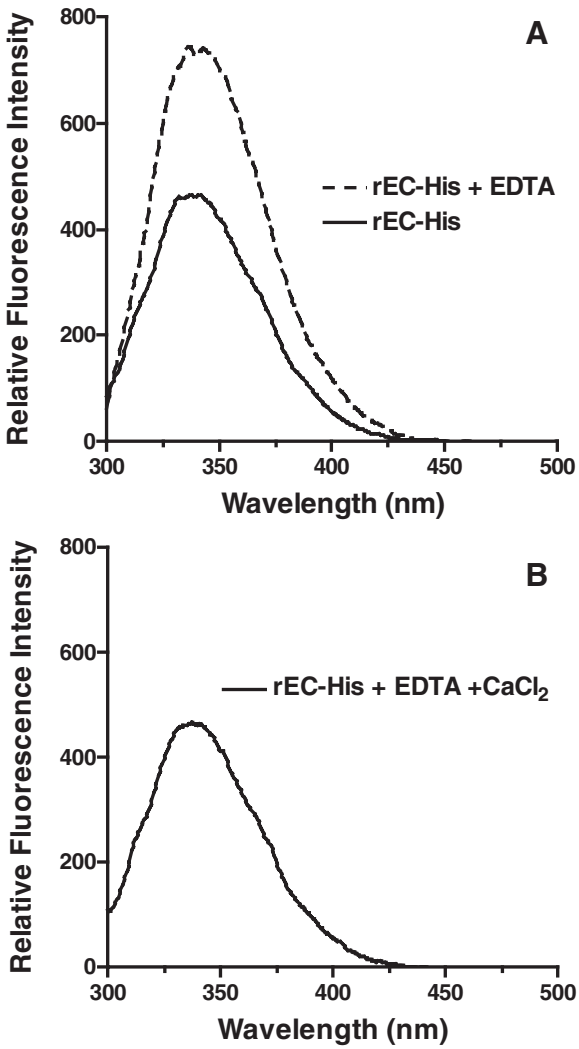

Fig. 5. Intrinsic ultraviolet fluorescent spectroscopy detects Ca^{+2}-dependent conformational changes of renatured rEC-His. Preparations of rEC-His for this assay involved saturation of rEC-His with Ca^{+2} followed by extensive dialysis to remove unbound Ca^{+2}. Spectra were obtained at an excitation wavelength of 280 nm. **A**: Spectra of rEC-His and rEC-His + EDTA. rEC-His was subjected to increasing concentrations of EDTA. **B**: Spectrum of rEC-His + EDTA + $CaCl_2$. To a separate sample that contained 0.025 mM EDTA, $CaCl_2$ was added to a final concentration of 0.05 mM. All spectra have been adjusted to remove the spectrum of the buffer in which rEC-His was dissolved.

To determine if this Ca^{2+}-dependent conformational change was reversible, Ca^{2+} was introduced back into the sample at a concentration that overcame the chelating properties of EDTA. rEC-His was observed to rebind Ca^{2+}, as demonstrated by its emission spectra that was nearly identical to the original sample (Fig. 5B). These Ca^{2+}-dependent shifts are consistent with fluorescence emission spectroscopy data of wild-type SPARC from mammalian cells (Engel et al., 1987) and rSPARC-His (Bassuk et al., 1996b).

Circular dichroism spectroscopy of renatured rEC-His

To further confirm the correct folding of renatured rEC-His, circular dichroism spectroscopy was used to detect the presence of a predominantly α-helical structure, which exists in the crystal structure of the EC domain (Hohenester et al., 1996). Preparations of rEC-His for this assay involved saturation of rEC-His with Ca^{2+} followed by extensive dialysis to remove unbound Ca^{2+}. Representative spectra of control rEC-His are shown in Figure 6A (solid line). Addition of Ca^{2+} (0.005–5 mM) to rEC-His yielded spectra indistinguishable from control spectra (data not shown), indicating that the original sample was already saturated with Ca^{2+}. Absorption at 220–225 nm is indicative of a secondary structure for rEC-His that is rich in α-helices. EDTA was added to a rEC-His sample at increasing concentrations to determine the extent to which α-helical secondary structure was dependent on bound Ca^{2+}. Addition of EDTA to a final concentration of 0.025 mM did not perturb the secondary structure of the protein to an appreciable degree (data not shown). However, the addition of EDTA to a final concentration of 0.25 and 2.5 mM resulted in a 22% and 50% decrease in absorption at 222 nm, respectively (Figure 6A,C). These results demonstrate that removal of bound Ca^{2+} from rEC-His by EDTA results in a significant loss of α-helical secondary structure and that Ca^{2+} is necessary for this structure. Figure 6B is a comparison between the spectra of rEC-His (solid line) and rSPARC-His (dashed line). The greater negative absorption at 222 nm for rEC-His confirms that a majority of the α-helices in SPARC exist in the EC domain, in agreement with previously published data of the secondary structure of SPARC (Engel et al., 1987) and the crystal structure of the EC domain (Hohenester et al., 1996).

Inhibition of urothelial cell spreading by rEC-His

Prior work from our laboratory (Hudson et al., 2005) demonstrated that spreading of freshly plated human urothelial cells was inhibited by rSPARC-His in a concentration- and time-dependent manner. To determine which domain of SPARC was responsible for anti-spreading activity, we tested preparations of rEC-His in spreading assays whereby the data were quantified through a Rounding Index (Bassuk et al., 1996a,b; Hudson et al., 2005). As a reference, the typical anti-spreading activity of rSPARC-His over 6 h is shown in Figure 7A. Figure 7B shows that spreading of the same bladder urothelial cell culture was also inhibited by rEC-His. The spreading of a different bladder urothelial cell culture was also observed to be inhibited by rEC-His in a concentration-dependent manner (Fig. 7C).

We also tested urothelial cells grown from a ureter, a mesodermally derived tissue that is embryologically distinct from endodermally derived bladder urothelium (Hudson et al., 2005). Figure 7D demonstrates that rEC-His was effective in inhibiting the spreading of ureteric

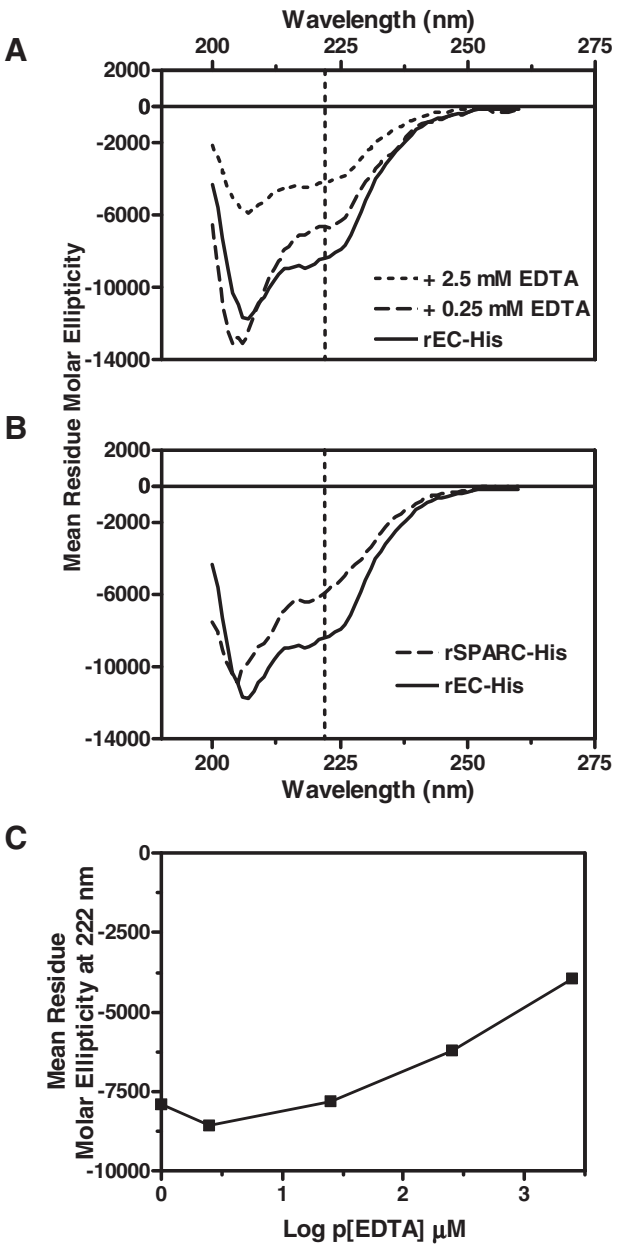

Fig. 6. Circular dichroism spectroscopy detects Ca^{+2}-dependent changes in α-helices of renatured rEC-His. **A**: Titration of rEC-His with EDTA. Shown are spectra for Ca^{+2}-saturated, control rEC-His (170 μg/ml, 8.9 μM, solid line), and two concentrations of EDTA as designated (2.5 mM EDTA, dotted line; 0.25 mM EDTA, dashed line). **B**: Comparison between rEC-His and rSPARC-His. rEC-His (170 μg/ml, 8.9 μM, solid line) and rSPARC-His (250 μg/ml, 7.8 μM, dashed line) were analyzed under the same conditions. Vertical dashed line in (A) and (B) designates observed values at 222 nm. **C**: Change in mean residue molar ellipticity of rEC-His at 222 nm as a function of EDTA concentration. Data points correspond to 0.25, 2.5, 25.0, 250.0, and 2,500.0 μM EDTA.

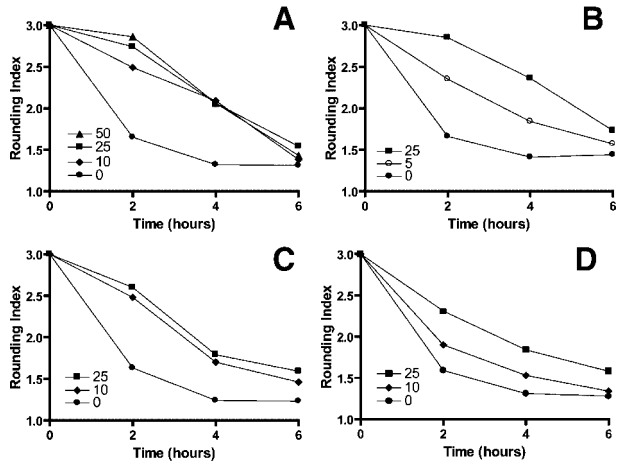

Fig. 7. Inhibition of urothelial cell spreading by rEC-His and rSPARC-His. Shown are spreading assay results derived from indices calculated as described in Materials and Methods. Proteins were added in increasing concentrations to cells and photographs were taken as described in Materials and Methods. **A**: Inhibition of normal bladder urothelial cell spreading by rSPARC-His. **B**, **C**: Inhibition of normal bladder urothelial cell spreading by rEC-His. **D**: Inhibition of normal ureteric urothelial cell spreading by rEC-His. SEM did not exceed 0.3 for all curves. See Materials and Methods for details of statistical analysis. Data in (A) reproduced from Hudson et al. (2005) with permission.

cells in a concentration- and time-dependent manner. It is noteworthy that endogenous SPARC is detected by immunohistochemistry in both bladder (Hudson et al., 2005) and ureteric (data not shown) urothelium.

The experiments performed with rEC-His were all highly similar in inhibition profiles and concentration-dependency. The collective data indicates that, like rSPARC-His (Hudson et al., 2005), rEC-His inhibits urothelial cells of different embryologically distinct origins (i.e., bladder urothelium from endoderm, and ureter urothelium from mesoderm). The results shown in Figure 7 indicate that the C-terminal extracellular Ca^{2+}-binding domain of SPARC (i.e., the "EC domain") confers anti-spreading activity to human urothelial cells.

Structural and biological activity of a point mutant in EF-hand 2 of rSPARC-His

To better understand the structural/functional relationship of the EC domain in conferring anti-spreading activity to SPARC, the properties of a point mutant constructed in EF-hand 2 was investigated. Substitution of the codon for E268 with a codon for F resulted in the generation of rSPARC(E268F)-His. E268 occupies the Z position of EF-hand 2 (Hohenester et al., 1996), and chelates Ca^{2+} with both oxygens of its side chain (Busch et al., 2000). Preparations of rSPARC(E268F)-His were evaluated by SDS–PAGE (Fig. 8A)—the polypeptide exhibited near identical electrophoretic mobilities under reducing (lane 2) and non-reducing (lane 4) conditions as rSPARC-His (lanes 1 and 3). Intrinsic UV fluorescence and circular dichroism spectroscopic assays of rSPARC(E268F)-His are shown in Figure 8B,C. Addition of EDTA and Ca^{2+} in increasing concentrations (0.0–2.5, 0.0–5.0 mM, respectively) resulted in minimal changes in relative fluorescence intensity and in mean residue molar ellipticity at 222 nm, as compared to rSPARC-His (Table 1), indicating that the high-affinity Ca^{2+}-binding properties of the protein that correlate with α-helical structure have been lost due to this point mutation. The mean residue molar ellipticity of rSPARC(E268F)-His at 222 nm was -3931 (Fig. 8C, solid line), a value 71% of that for rSPARC-His (Fig. 8C, stippled line).

rSPARC(E268F)-His was also examined for anti-spreading activity. Over the range of rSPARC(E268F)-His studied (0, 10, 25, and 50 μg/ml), the mutated protein lacked the ability to inhibit the spreading of urothelial

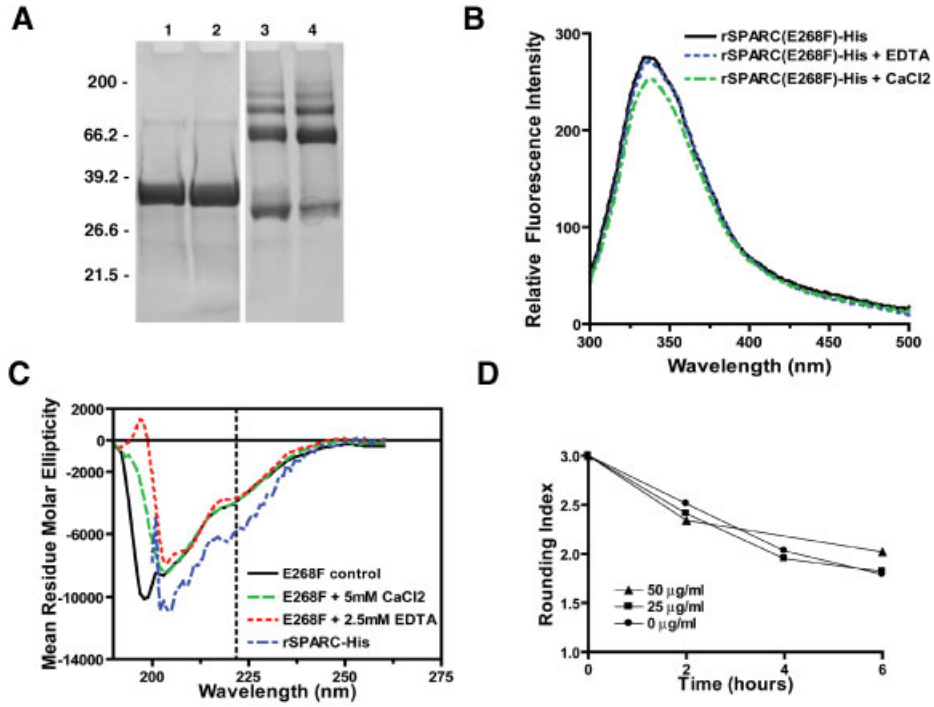

Fig. 8. Isolation, conformation, and biological activity of the mutant rSPARC(E268F)-His. **A**: Isolation and renaturation of rSPARC (E268F). Shown is a polyacrylamide gel that contained 0.1% SDS of rSPARC-His (lanes 1 and 3) and rSPARC(E268F)-His (lanes 2 and 4) under reducing (lanes 1–2) and non-reducing conditions (lanes 3–4). **B**: Intrinsic ultraviolet fluorescent spectroscopy. Shown are spectra for control rSPARC(E268F)-His (40 µg/ml, solid line), rSPARC(E268F)-His with 0.5 M EDTA (dotted line), and rSPARC(E268F)-His with 7.5 mM $CaCl_2$. **C**: Circular dichroism. Shown are spectra for control rSPARC(E268F)-His (300 µg/ml, solid line), rSPARC(E268F)-His with 2.5 mM EDTA (dotted line), rSPARC(E268F)-His with 5 mM $CaCl_2$ (dashed line), and rSPARC-His (stippled line). **D**: Urothelial cell spreading is not inhibited by SPARC(E268F)-His. Ureteric urothelial cell cultures, passage 3, were subjected to varying concentrations of rSPARC(E268F)-His. Data points for input recombinant proteins (in µg/ml) are as follows: closed circle, 0; closed square, 25; closed triangle, 50. SEM did not exceed 0.3. See Experimental Methods for details of statistical analysis.

cells (Fig. 8D). This lack of anti-spreading activity, which was dissimilar to that observed for rEC-His and rSPARC-His (Fig. 7), provides evidence that the motif of SPARC responsible for this activity was dependent on the coordination of Ca^{2+} by a Glu residue at the Z position of EF-hand 2.

DISCUSSION

Development of new therapeutic reagents to facilitate the healing of urothelial wounds would be highly advantageous in the clinical management of bladder abnormalities that include bladder exstrophy, neurogenic bladders, interstitial cystitis, and trauma. Such reagents would need to improve the efficiency of grafts by modulating the migration and spreading of urothelial cells. Candidate proteins to fulfill these requirements would be expected to exhibit counteradhesive properties that include the ability to dismantle focal adhesions. Such a candidate protein is SPARC, a 43 kDa metalloprotein that exhibits a remarkable ability to traffic either into urothelial cell nuclei or into the extracellular space (Hudson et al., 2005).

TABLE 1. Comparison of the calcium induced changes among rSPARC-His, rEC-His, and rSPARC(E268F)-His

Protein	Experimental method	ΔF_{336} (%)[a]	$\Delta[\theta]_{222}$ (%)[b]
rSPARC-His	EDTA titration	74.0	50.0
rEC-His	EDTA titration	61.0[c]	50.0[d]
rSPARC(E268F)-His	EDTA titration	1.8[e]	5.6[f]

[a]Change in relative intrinsic UV fluorescence at 336 nm, calculated from signals of Ca^{2+}-saturated and EDTA-treated proteins according to the formula (saturated-treated)/saturated.
[b]Change in mean residue molar ellipticity at 222 nm, calculated from signals of Ca^{2+}-saturated and EDTA-treated proteins according to the formula (saturated-treated)/saturated.
[c]Figure 5a.
[d]Figure 6a.
[e]Figure 8b.
[f]Figure 8c.

Despite a wealth of information on the structural and biophysical properties of SPARC (Sage et al., 1995; Bassuk et al., 1996a,b; Hohenester et al., 1996; Hohenester et al., 1997; Sasaki et al., 1998; Busch et al., 2000), minimal analogous information exists for the anti-spreading activity of SPARC. Our assignment of this activity to the EC domain advances the field by permitting new insights into the Ca^{2+}-dependent activity of this multidomain protein. The expression of SPARC and EC protein in *E. coli* has provided additional insights into the renaturation of these two recombinant proteins. Preparations of rSPARC-His have been realized in high yields (>70 mg/10 L) and shown to be folded into a conformation that is biologically active (Bassuk et al., 1996a,b; Sage et al., 2003). With this knowledge, we decided to produce the recombinant EC domain of SPARC in the BL21(DE3) *E. coli* vector in order to obtain large quantities of the recombinant protein. However, isolation of rEC-His was not as straightforward as anticipated. While soluble forms of the EC protein have been obtained from eukaryotic expression systems (Schiemann et al., 2003), the bacterial recombinant protein was predominantly insoluble. This can be attributed to the fact that prokaryotic cells do not contain organelles that function in post-translational modification. In order to obtain an isolated, renatured form of rEC-His, it was necessary to perform the following series

of steps. The protein had to be completely denatured with urea and isolated utilizing its strong binding to metal-chelate affinity chromatography resins. While it was possible to remove denaturing conditions and refold rSPARC-His when bound to the chromatography column (Bassuk et al., 1996b), attempts to duplicate the procedure with rEC-His were unsuccessful, suggesting that the protein precipitated in the column prior to elution. Instead, rEC-His protein had to be eluted from the column in the denaturing solution and refolded using a series of dialysis steps that slowly removed the denaturing conditions while slowly introducing disulfide isomerization and Ca^{2+}-dependent refolding conditions—all while preventing Ca^{2+} salts from precipitating from the solution. This procedure was capable of producing large amounts (>70 mg/10 L) of the recombinant protein. These high yields were beneficial in performing the biochemical and biological experiments reported here—especially since most of the assays were from the same recombinant protein preparation.

The conclusion that rEC-His is correctly folded into a functional polypeptide domain is based on the results from intrinsic UV fluorescence and circular dichroism spectroscopic assays. These intrinsic UV fluorescence assays are an indicator of the environment surrounding the 3 Trp of SPARC, of which all reside in the EC domain (Hohenester et al., 1996). Because the observed intrinsic fluorescence patterns of rSPARC-His (Bassuk et al., 1996b) and rEC-His (Fig. 5) were equally responsive to Ca^{2+} and EDTA, preparations of rEC-His, therefore, existed as both a structural and functional domain polypeptide. Correspondingly, the circular dichroism spectroscopic assays are an indicator of the presence of the α-helices of SPARC, of which most reside in the EC domain (Hohenester et al., 1996). While α-helices are predicted to occur in the N-terminal domain I of SPARC by secondary structure considerations (Engel et al., 1987; Bassuk et al., 1993), the extent to which domain I contains α-helices is not known because it has escaped crystallization due to its flexibility in solutions (Hohenester et al., 1996). The α-helical conformations of SPARC (Bassuk et al., 1996b) and EC (Fig. 6), as determined by the mean residue molar ellipticity at 222 nm, were equally responsive to Ca^{2+} and EDTA—further supporting the conclusion that rEC-His exists as a structural and functional domain polypeptide. The consistency in the properties of renatured rEC-His was supported by equivalent ability of rSPARC-His and rEC-His to inhibit urothelial cell spreading in concentration- and time-dependent manners.

Under physiological conditions, SPARC and the EC domain is Ca^{2+}-saturated due to a K_d of 57–490 and 56–11,750 nM, respectively, for the high-affinity Ca^{2+}-binding EF-hand motifs (Busch et al., 2000). Because urothelial cell cultures require exogenous Ca^{2+} for viability (Southgate et al., 1994) (data not shown), it was not possible to assay Ca^{2+}-deficient rSPARC or Ca^{2+}-deficient rEC-His in spreading assays performed in Ca^{2+}-deficient media. We therefore generated, and tested, an rSPARC-His mutant deficient in Ca^{2+}-dependent structural and functional activities. The conformation of rSPARC(E268F)-His was not responsive to addition or depletion of Ca^{2+}, a result consistent with the contribution of EF-hand 2 to the Ca^{2+}-binding properties of SPARC. The lack of anti-spreading activity of rSPARC(E268F)-His indicates that this activity depends on the EF-hand 2 motif. The collective evidence yields novel insights about the specialized functions of the third domain of SPARC.

rEC-His was observed to inhibit the spreading of two, embryologically distinct types of urothelial cells—bladder (endoderm) and ureter (mesoderm). This result is consistent with similar observations for rSPARC-His (Hudson et al., 2005) and illustrates the mechanism by which SPARC participates in adhesive forces that drive urothelial development, homeostasis, and the response to injury.

ACKNOWLEDGMENTS

We acknowledge Brad McMullen and Dr. Earl Davie for N-terminal amino acid sequencing by Edman degradation, Elizabeth Leaf for fermentations, Kristy Seidel for expert statistical analysis, the Howard Hughes Undergraduate Research Program (C.F.D.), the Mary Gates Endowment for Students Research Training Grant (A.E.H.), a University of Washington Institutional National Research Service Award NIDDK T32 DK07779 (J.K.), a Pediatric Urology Fellowship from the Residency Review Committee for Urology (W.C.F.), and support from NIDDK R01DK58881 (J.A.B.).

LITERATURE CITED

Adams JC, Watt FM. 1993. Regulation of development and differentiation by the extracellular matrix. Dev Suppl 117:1183–1198.

Bassuk JA, Iruela-Arispe ML, Lane TF, Benson JM, Berg RA, Sage EH. 1993. Molecular analysis of chicken embryo SPARC (osteonectin). Eur J Biochem 218:117–127.

Bassuk JA, Baneyx F, Vernon RB, Funk SE, Sage EH. 1996a. Expression of biologically active human SPARC from *Escherichia coli*. Arch Biochem Biophys 325:8–19.

Bassuk JA, Braun LP, Motamed K, Baneyx F, Sage EH. 1996b. Renaturation of SPARC expressed in *Escherichia coli* requires isomerization of disulfide bonds for recovery of biological activity. Int J Biochem Cell Biol 28:1031–1043.

Bolander ME, Young MF, Fisher LW, Yamada Y, Termine JD. 1988. Osteonectin cDNA sequence reveals potential binding regions for calcium and hydroxyapatite and shows homologies with both a basement membrane protein (SPARC) and a serine proteinase inhibitor (ovomucoid). Proc Natl Acad Sci USA 85: 2919–2923.

Busch E, Hohenester E, Timpl R, Paulsson M, Maurer P. 2000. Calcium affinity, cooperativity, and domain interactions of extracellular EF-hands present in BM-40. J Biol Chem 275:25508–25515.

Crowe J, Dobeli H, Gentz R, Hochuli E, Stuber D, Henco K. 1994. 6xHis-Ni-NTA chromatography as a superior technique in recombinant protein expression/purification. Methods Mol Biol 31:371–387.

Davidson WS, Arnvig-McGuire K, Kennedy A, Kosman J, Hazlett TL, Jonas A. 1999. Structural organization of the N-terminal domain of apolipoprotein A-I: Studies of tryptophan mutants. Biochemistry 38:14387–14395.

Edman P, Begg G. 1967. A protein sequenator. Eur J Biochem 1:80–91.

Engel J, Taylor W, Paulsson M, Sage H, Hogan B. 1987. Calcium-binding domains and calcium-induced transition in SPARC (osteonectin/BM-40), an extracellular glycoprotein expressed in mineralized bone and nonmineralized tissues. Biochemistry 26:6958–6965.

Gumbiner BM. 1996. Cell adhesion: The molecular basis of tissue architecture and morphogenesis. Cell 84:345–357.

Hay ED. 1981. Extracellular matrix. J Cell Biol 91:205s–223s.

Hochuli E. 1990. Purification of recombinant proteins with metal chelate adsorbent. Genet Eng (NY) 12:87–98.

Hochuli E, Dobeli H, Schacher A. 1987. New metal chelate adsorbent is selective for proteins and peptides containing neighbouring histidine residues. J Chromatography 411:177–184.

Hohenester E, Maurer P, Hohenadl C, Timpl R, Jansonius JN, Engel J. 1996. Structure of a novel extracellular Ca+2-binding module in BM- 40/SPARC/osteonectin. Nat Struct Biol 3:67–73.

Hohenester E, Maurer P, Timpl R. 1997. Crystal structure of a pair of follistatin-like and EF-hand calcium-binding domains of BM-40. EMBO J 16:3778–3786.

Hudson AE, Feng WC, Delostrinos CF, Carmean N, Bassuk JA. 2005. Spreading of embryologically distinct urothelial cells is inhibited by SPARC. J Cell Physiol 202:453–463.

Ingber DE. 1993. The riddle of morphogenesis: A question of solution chemistry or molecular cell engineering? Cell 75:1249–1252.

Juliano RL, Haskill S. 1993. Signal transduction from the extracellular matrix. J Cell Biol 120:577–585.

Lane TF, Sage EH. 1994. The biology of SPARC, a protein that modulates cell-matrix interactions. FASEB J 8:163–173.

Maurer P, Mayer U, Bruch M, Jeno P, Mann K, Landwehr R, Engel J, Timpl R. 1992. High and low affinity calcium binding and stability of the multi-domain extracellular glycoprotein BM-40/SPARC/osteonectin. Eur J Biochem 205: 233–240.

Maurer P, Hohenadl C, Hohenester E, Gohring W, Timpl R, Engel J. 1995. The C-terminal portion of BM-40 (SPARC/Osteonectin) is an autonomously folding and crystallisable domain that binds calcium and collagen IV. J Mol Biol 253: 347–357.

Miller R. 1986. Beyond Anova, Basics of Applied Statistics. New York: John Wiley and Sons. pp 43–44.

Motamed K, Bassuk JA, Sage EH. 1995. Anti-adhesive properties of SPARC: Structural and functional correlates. In: Crossin KL, editor. Tenascin and other counteradhesive molecules of the extracellular matrix. Amsterdam: Harwood Academic Press. pp 111–131.

Romberg RW, Werness PG, Lollar P, Riggs BL, Mann KG. 1985. Isolation and characterization of native adult osteonectin. J Biol Chem 260:2728–2736.

Sage H, Vernon RB, Funk SE, Everitt EA, Angello J. 1989. SPARC, a secreted protein associated with cellular proliferation, inhibits cell spreading in vitro and exhibits Ca+2-dependent binding to the extracellular matrix. J Cell Biol 109:341–356.

Sage EH, Bassuk JA, Yost JC, Folkman MJ, Lane TF. 1995. Inhibition of endothelial cell proliferation by SPARC is mediated through a Ca+2-binding EF-hand sequence. J Cell Biochem 57:127–140.

Sage EH, Reed M, Funk SE, Truong T, Steadele M, Puolakkainen P, Maurice DH, Bassuk JA. 2003. Cleavage of the matricellular protein SPARC by matrix metalloproteinase 3 produces polypeptides that influence angiogenesis. J Biol Chem 278:37849–37857.

Sasaki T, Hohenester E, Gohring W, Timpl R. 1998. Crystal structure and mapping by site-directed mutagenesis of the collagen-binding epitope of an activated form of BM-40/SPARC/osteonectin. EMBO J 17:1625–1634.

Schiemann BJ, Neil JR, Schiemann WP. 2003. SPARC inhibits epithelial cell proliferation in part through stimulation of the transforming growth factor-beta-signaling system. Mol Biol Cell 14:3977–3988.

Schmitt E, Guillon JM, Meinnel T, Mechulam Y, Dardel F, Blanquet S. 1996. Molecular recognition governing the initiation of translation in *Escherichia coli*. A review. Biochimie 78:543–554.

Schneider EL, Thomas JBJA, Sage EH, Baneyx F. 1997. Aggregation and disulfide bond formation in recombinant human SPARC synthesized in the cytoplasm of wild type and trx B *Escherichia coli*. Nature Biotech 15:581–585.

Shibanuma M, Mashimo J, Mita A, Kuroki T, Nose K. 1993. Cloning from a mouse osteoblastic cell line of a set of transforming-growth-factor b1-regulated genes, one of which seems to encode a follistatin-related polypeptide. Eur J Biochem 217:15–19.

Southgate J, Hutton KA, Thomas DF, Trejdosiewicz LK. 1994. Normal human urothelial cells in vitro: Proliferation and induction of stratification. Lab Invest 71:583–594.

Termine JD, Kleinman HK, Whitson SW, Conn KM, McGarvey ML, Martin GR. 1981. Osteonectin, a bone-specific protein linking mineral to collagen. Cell 26: 99–105.

Yost JC, Bell A, Seale R, Sage EH. 1994. Purification of biologically active SPARC expressed in *Saccharomyces cerevisiae*. Arch Biochem Biophys 314:50–63.